Investigation of Lithium-ion Battery Cycling in a Grid-tied Rooftop PV System through Accelerated Testing

Aditya Nadkarni, *Student Member*, *IEEE*, George G. Karady, *Fellow, IEEE,*

Ken Alteneder. *Salt River Project*

***Abstract*— Residential battery energy storage is expected to add considerable value to urban rooftop PV systems under Time-of-Use (TOU) retail electricity tariff structures. Lithium ion batteries in particular could provide an efficient means of shaving residential seasonal evening peak demand. In this paper, daily cycling behavior of a 73 Watt-hour (Wh) prototype lithium ion battery is analyzed on an accelerated basis to study its daily cycling characteristics as in a PV coupled system. Summer specific cycling of storage battery is conducted with a variable resistive load bank and a PWM controlled DC power supply substituting solar array. Due to the accelerated nature of testing, four round trips were possible in a single day. The battery was able to supply 1.21 kWh of monthly and 40 Wh of daily summer load with 45 Wh average input in each charging cycle. Economic and system indices driving monthly electricity charge savings are also addressed.**

***Index Terms*—Energy storage, Batteries, Photovoltaic systems, Test facilities, retail energy prices**

I. INTRODUCTION

With continuous innovation in stationary storage technology and automation advancements in distribution system load management equipment, battery storage is expected to enhance savings from grid tied photovoltaic (PV) systems. Lithium ion batteries with their high energy densities are being increasingly used in battery assisted PV systems. Domestic owners of such systems benefit from reducing their on-peak grid power consumption. Also, greater number of customers discharging their stored energy on peak, in turn, has the capacity to ease heavy loading on utility substation transformer. These effects are particularly realized during summer when the distribution substation has to serve the annual peak demand. In view of this, utilities can motivate installation of energy storage in the customer premises. However, capital cost of the entire system and payback period remain some of the major prohibitive concerns. Moreover, Lithium ion batteries are affected by cycle life degradation or ageing and its effects are realized over a period of 4-7 years under different cycling conditions [1]. Disposal of a large number of such aged batteries could also pose environmental hazards. However from the operational perspective, if the excess PV energy produced during daytime in summer is routed to charge the storage, evening demand peak can be shaved. This is expected to yield greater returns as the on-peak retail prices are much higher than the energy buyback credits earned. As daily average sunshine hours and customer behavior towards electricity usage vary from place to place, a location specific study of battery cycling becomes imperative to estimate these benefits.

Stationary battery cycling tests were carried out in [2] for a typical household in Arizona in order to have a long term perspective on the battery performance from the actual field. Similar field testing of batteries generally takes a long time (3-5 years) for the results to be available. An indoor testing method closely replicating a PV system could therefore be desirable for accelerated, flexible and controllable assessment of battery sizing and savings from its operation [3-7]. In the recent past, Agilent Technologies's 'Solar Array Simulator' or SAS has been used as a laboratory substitute for PV panels for matching batteries to PV panel peak rating in stand-alone applications [6,7]. A design of Stand-alone system in Malaysia with real time solar data is discussed in [8] while in [9], a smart charge technique for reducing electricity bills is discussed although without a PV element. However, in all these indoor methods, actual month long experimental verification of battery cycling with regards to seasonal variations has not been performed. Also, no particular charging and discharging strategies in response to the retail tariff plans were addressed.

It is perceived that use of adequately sized batteries and a supporting tariff structure would help reduce the rating of rooftop PV, thereby reducing the overall system cost. This paper proposes a simple low cost method to incorporate accelerated laboratory testing of Lithium ion batteries to experimentally verify their cycling behavior and dispatch of stored energy. The cycling strategy discussed here is motivated by the fact that spring and summer in Arizona, invariably see enough excess PV output in the morning which can be conveniently stored and used to maximize on-peak energy savings thereby completely eliminating the off-peak

charging costs. The indoor system built for the study is seen as a small scale replication of actual on-line system. With the accelerated testing method described, it was possible to have the battery closely follow the charging pattern from a PV source as in the field. Testing was conducted with summer specific charge/discharge profiles on a prototype 73 Wh Lithium ion battery. For storage dispatch, a typical residential load profile in Arizona seen with Salt River Project (SRP) tariff plan E-26 was implemented [10]. Also, ability of the system to recover from a low state of charge to full charge following insufficient charging was analyzed.

The paper is organized as follows. Section II describes the battery cycling strategy adopted. Section III explains the experimental hardware setup to carry out the proposed accelerated testing. Results from the cycling tests with regards to battery performance are elaborated in section IV followed by identification of cost-savings factors in comparison to other PV and grid-tied storage system configurations in section V. Important conclusions and scope for future research are given in Section VI.

II. HOURLY BATTERY CYCLING STRATEGY

The average summer PV output, customer demand corresponding to E-26 TOU plan and battery profile corresponding to 40% peak shave target are shown in Fig.1. The hourly retail electricity prices are also shown with bars [11]. It can be observed that peak PV output and peak demand are displaced in time and summer PV output is in excess during the daytime for six hours atleast.

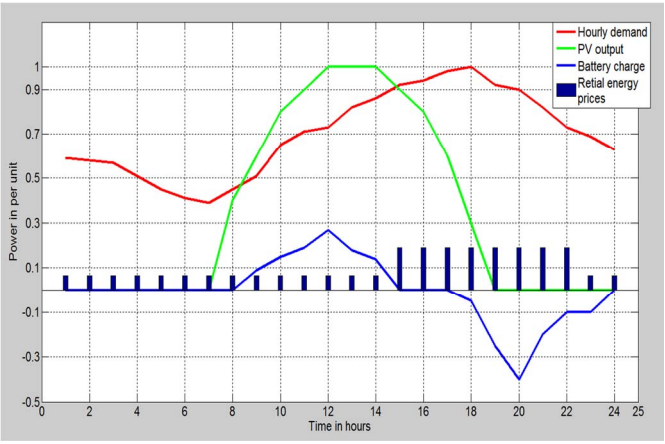

Figure 1: Hourly PV, demand and battery cycling profile for summer

The battery charge equation is given by (1)

$$P_{battery} = P_{PV} - P_{demand} \quad (1)$$

Where, $P_{battery}$ is the charge received by the battery in per unit, P_{PV} is the output of PV system in per unit and P_{demand} indicates hourly customer demand in per unit. Taking into account the tariff structure, load and PV profile, the following cycling method can be adopted in a real on-line system [10].

1. From 8 am in the morning to 3 pm in the afternoon, the excess energy after mitigating the hourly residential demand can be used to charge the battery rather than being sent back to the grid.
2. Charging should be halted at 3 pm when on-peak hours begin even if excess PV output persists. All the available energy from PV is then routed to meet the house demand as the energy prices are highest during this period.
3. For hours 3 pm onwards until 8 pm, if the demand exceeds peak-shave target, storage is dispatched with its available charge to help cut down the peak to the pre-determined peak shave target
4. If the battery has surplus charge at the end of on-peak hours, it can be used in the subsequent off-peak hours.

This methodology was practiced on a back to back basis using an artificial PV source thereby closely replicating actual system in practice. Testing was done with respect to summer PV and load behavior only, as the battery sized for summer cycling is expected to be adequate for winter time demand.

III. EXPERIMENTAL SETUP

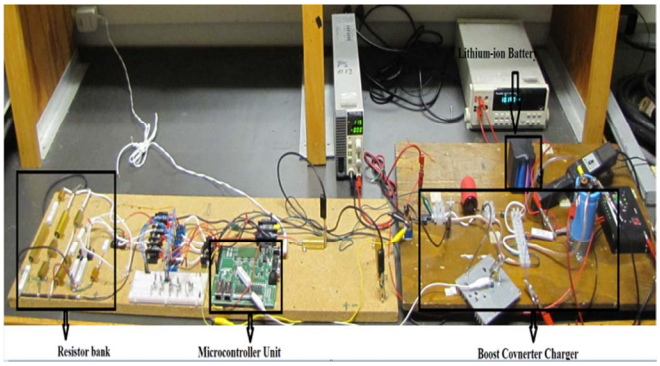

Figure 2: Testing experimental setup in the laboratory

Shown in Fig.2, the test bed consists of four principle sections, namely, the lithium ion battery, the artificial PV source and a boost converter circuit, a resistive load bank for battery discharge and a central microcontroller unit (MCU) which governs daily cycling of the system. Labview data acquisition system was employed to sample battery input/output current, voltage and power data on one minute basis. Testing was carried out indoors where an ambient temperature of 25^0C was maintained. Unlike a similar implementation as in [5], the focus of this work was more on the aggregate energy flow in and out of the battery. Operating

characteristics of each of these sections are described below in detail.

A. Lithium ion battery

Important specifications of the Lithium-ion battery used as a prototype in testing are listed in Table I. Cycling characteristics observed with the prototype battery based on these specifications can be extended to large capacity batteries actually implemented in practice.

Table I: Test battery parameters

Battery parameters	**Recommended values**
Battery pack configuration	9 cells (3x3)
Battery pack nominal voltage	11.1 V
Battery pack peak voltage	12.6 V
Capacity	73.26 Wh, 6.6 Ah
Max discharge rate	7.0 A
Low voltage indicator	9.6 V
Low voltage disconnect	8.5 V
Overvoltage disconnect	13.0 V

B. Battery charging module

The battery charging module consisted of a laboratory DC power supply, boost converter circuit and a PIC 18F97J60 microcontroller (MCU) with an inbuilt Pulse width modulation (PWM) module. The boost converter stepped up the DC source voltage from a preset 11.5 V to a value determined by the duty cycle programmed in MCU which controlled the charge flow into the battery terminals. Steps implemented to determine power input to the battery are explained below.

1. With 11.5 V set at the boost converter input, battery current and power input were calculated using (2,3).

$$I_{charge} = \frac{V_{Charge} - V_{batt}}{R_{batt}} A \quad (2)$$

$$P_{charge} = V_{charge} * I_{charge} W \quad (3)$$

$$D = \frac{(V_{charge} - 11.5)}{V_{charge}} \% \quad (4)$$

Where, I_{charge}, V_{Charge}, P_{charge} are battery charging current, voltage and power respectively. V_{batt} is the instantaneous battery terminal voltage. D indicates the PWM duty cycle value while R_{batt} is the internal resistance of the battery in ohms.

2. I_{charge} was limited to 1.7 A (0.25C) as per the manufacturer's recommended battery charging rate. Maximum charging output of the boost converter and the maximum duty cycle were thus limited to about 20 W and 12% respectively as determined by (2) ,(3) and (4). Each charging step was of 30 minutes.

3. The hourly demand following an established pattern in every round-trip of cycling similar to shown in Fig. 1. Also, per unit hourly PV output closely follows the variations in hourly insolation given in Wh/m^2. 2004 hourly summer insolation data obtained from NREL's National Solar Radiation Data Base (NSRDB) was normalized to a base of 1000 Wh/m^2 using (5) [12]. The charging energy in per unit of peak P_{charge} was then obtained from (1). Duty cycle input of PWM corresponding to P_{charge} is given in (6).

$$P_{PV} = \frac{S}{1000} \quad (5)$$

$$D = P_{battery} * D_{max} \quad (6)$$

Where, S is the hourly solar irradiance in Wh/m^2 and D_{max} is 12% as from step 1, P_{PV} is expressed in per unit .

4. With this configuration, it was possible to charge the battery with the amount of watts in every charging step as dictated by the programmed duty cycles. Any charging pattern could thus be reproduced if charging peak rating was known.

For the boost converter circuit, a 200 uH inductor and 220 uF capacitor were selected in order to have output current ripple within 10% and output voltage ripple within 5% of their ratings. An EPHC – Smart DC voltage controller was used to indicate if the battery level was full, the battery was being overcharged or was completely discharged. The microcontroller PWM unit was programmed using PICkit-3 and its frequency was set at 100 kHz.

C. Battery discharge module

The MCU switched between charge and discharge modes by operating a simple relay, thereby making the system work continuously once put to operation. In order to replicate a six step discharge (3 pm – 9 pm), a switching resistor bank was constructed. The battery was allowed to discharge into the bank with the load switched every 30 minutes. Each of the six legs of the resistor bank had a DC relay with a 3V DC coil. They were operated in response to the signals from the MCU register bits set as 0 or 1. Similar to the charging current, the maximum discharge current supplied to the load was limited

to 2.25 A (0.3 C). The maximum possible power output of battery is given by (7).

$$P_{(o)max} = V_{battery,avg} * I_{discharge,max} = 25\ W \qquad (7)$$

Where, $P_{(o),max}$ denotes the maximum output of the battery in Watts, $V_{battery,avg}$ is the average discharge voltage (about 11.1 V) of the battery at maximum discharge rate and $I_{discharge,max}$ is the maximum discharge current of 2.25 A. With different switching combinations of resistor bank, it was possible to reproduce the discharge loadshape by switching appropriate branches. The system was operated in Back to back charge and discharge modes following signals from the MCU unit.

Fig. 3 depicts the reproduction of expected cycling profile for battery cycling using the controlled DC voltage source and load bank. The right plot in Fig. 3 indicates the expected variation in cycling whereas the left plot suggests actual cycling profile observed. It should be noted that in every 30 minute charging step, the one minute power reading remained within 5% of its starting value. Positive values in the figure indicate charging whereas negative values indicate discharging of the battery. The cycling hours indicate total number of hours for which one round-trip cycle lasts.

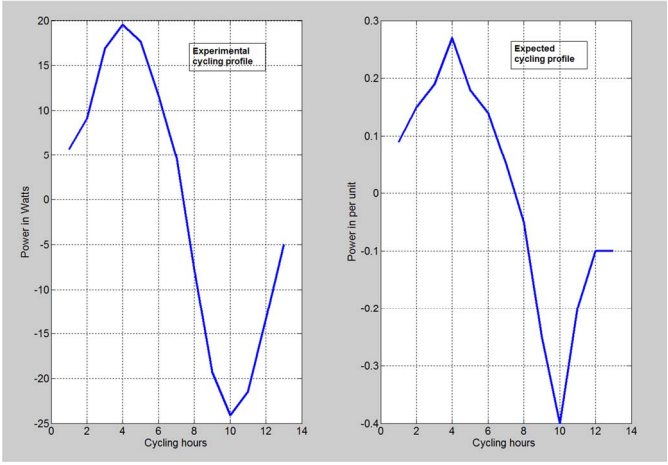

Figure 3: Comparison of reproduced and expected battery cycling profiles

D. Data acqusition system

NI-6025E (DAQ) with NI-SCXI-1000 power conditioner was used as the data acquisition system to continuously record instantaneous battery current, voltage and power. A Tektronix A622 AC/DC current probe was used to sense battery current/voltage and provide them to the LabView DAQ. The data thus obtained was processed in MATLAB to plot salient results.

IV. TEST RESULTS

With each round trip of battery cycling taking approximately six hours, one day of testing provided four days' data. Minute by minute data of battery terminal voltage and current from each cycle were processed to determine the following parameters

1. Average daily charge and discharge energies in Wh
2. Monthly charging and discharging energies in Wh
3. 30 minute average power intake and dispatch of the battery unit.
4. State of charge of the battery during its cycling

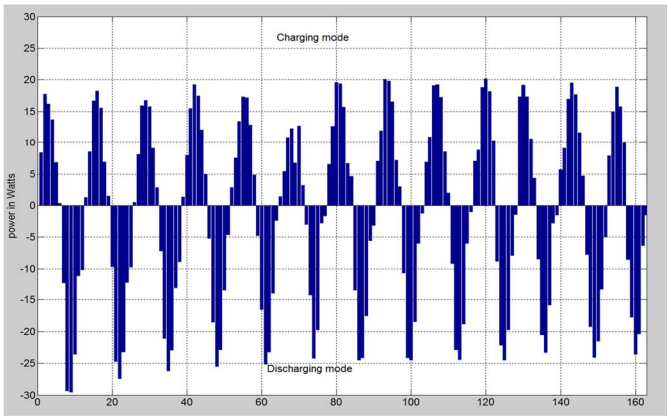

Figure 4: Average charging and discharging power observed in each step of cycling

Average charging Wh reading for a round-trip was about 45 Wh with the programmed charging profile. 30 minute average power consumed and dispatched by the battery during its cycling is shown in Fig. 4. Variations in the average charging power in each step are reflective of the variability in the excess PV power produced on hourly basis every day. The variability was due to proportional real time irradiance parameter introduced in microcontroller duty cycle control fucntion.The first battery discharge began with the battery state of charge at 100% resulting in higher dispatch. However, as the cycling progressed, the peak dispatch settled to about 25 W as given by (7).

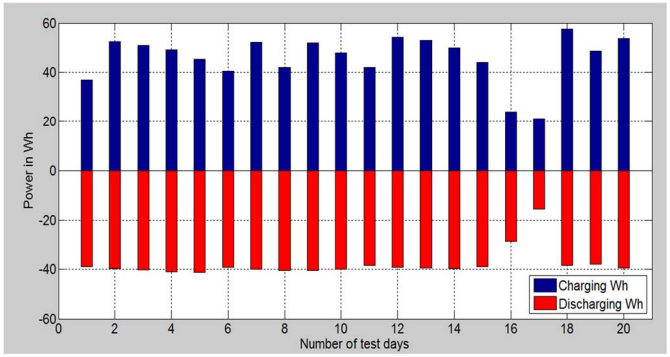

Figure 5: Daily Wh profile of battery cycling

Further, a 30 cycle test was performed to assess the ability of the battery to sustain the 40 Wh daily load on an average. Charging and discharging Wh for 20 days are shown in Fig. 5. It was seen that inspite of considerable variability in PV charging of the battery, it was able to supply about 40 Wh of energy on daily basis. Corresponding to day 16 and 17 cycling, due to insufficient charging of the battery, it was completely depleted post its discharge. Enough charging in subsequent cycles ensured that the battery regained its charge.

Table II enlists some of the major performance parameters observed during the month long cycling.

Table 2: Summary on monthly battery cycling performance

System performance parameters	**Summer (July)**
Total 30 cycle Wh output	1210.7
Average Wh output per cycle	40.05
Average peak power output in W	25
Total 30 cycle Wh input	1470.5
Average Wh input per cycle	45.43
Maximum battery SOC (%)	92.5 (Cycle 3)
Minimum battery SOC (%)	20 (cycle 25,26)
Average battery SOC (%)	63.1

V. FACTORS AFFECTING MONTHLY SAVINGS

A. *Present system against a PV-alone system*

Results are shown below for a real-world system with 2 kW peak demand, 2kW/4.4 hour storage and 40% peak-shave target. This system implements the topology proposed in this paper in which both PV and storage components are present. Fig. 6 (Left) shows monthly savings on the electricity bill (E-26) for a customer with 3.75 kW PV whereas Fig. 6 (Right) depicts comparison of annual electricity bill with a PV-alone system and a battery assisted PV system with various PV sizes. The red line or the basebill ($766) is the annual electricity bill incurred if no PV or storage system was installed.

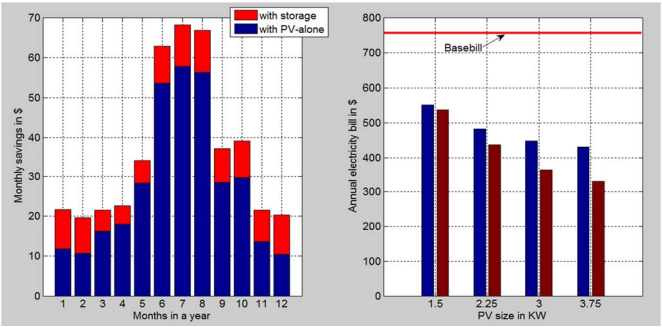

Figure 6: Monthly and annual revenue with respect to E-26 tariff

In comparison to a grid-tied PV-alone system, peak shaving with storage becomes a valuable proposition to the customer due to the price differential in the energy buyback or net metering credits earned and on-peak electricity prices. SRP net metering credits are earned such that every unit of energy sent to the grid is credited with the average annual on-peak electricity price at Palo-Verde [12]. Peak shaving savings at the same time are realized as the savings on on-peak prices which in the case of E-26 are $0.1913/unit. Difference between energy buyback or net metering credits and savings from peak shaving for the same amount of excess energy produces is given in (8)

$$S_{peak-shave} = (C_{on-peak} - C_{Netmet}) * P_{batt} \quad (8)$$

Where, $S_{peak-shave}$ are the savings in $ exceeding those earned from net metering or buyback. $C_{on-peak}$ denotes on-peak retail energy price in $/unit. Also, C_{Netmet} is the average annual on-peak market price in $/unit and P_{batt} is the amount of energy in per unit produced in excess of hourly demand.

B. *Present system against a storage-alone system*

For an equally sized storage system without any PV component, benefits of peak-shaving can be realized in the same fashion. As there is no PV energy involved, the storage needs to be charged with the grid energy during off-peak hours. Hence, for the same amount of peak-shaving, savings from the proposed configuration in comparison to that with off-peak charging can be given as in (9)

$$S_{peak-shave} = C_{off-peak} * P_{batt} \quad (9)$$

Where $C_{off-peak}$ = Off-peak retail electricity price in $/unit. Other terms are similar to those in (8). In the configuration without a PV component, the storage can be charged fully every day and its charging is independent of PV variability.

In view of this, it can be concluded that the major factors contributing to the benefits from the proposed configuration of storage and PV are

1. On-peak and energy buyback price differential
2. On-peak and off-peak price differential
3. Round trip efficiency of the storage
4. Customer demand behavior during off-peak periods

Higher values of the first three quantities in the above list and lower values on the fourth would yield more benefits from the proposed cycling strategy compared to other system configurations.

VI. CONCLUSION

Summer specific testing of a prototype Lithium ion battery was carried out on an accelerated basis. The battery was subjected to charging and discharging duties similar to those in a typical rooftop PV system. Daily and monthly cycling capacities and ability to respond to variations in charge were assessed. A method was developed to provide and obtain precise amounts of watts and watt-hours through battery cycling. The 73 Wh battery was able to sustain a daily demand of 40 Wh with 45 Wh average charging in every cycle. The battery state of charge varied widely from 20% to about 90% in response to variations in charging energy. Finally, the economic viability of the proposed configuration was addressed in comparison to individually operated PV and storage systems. It was observed that, in a place like Arizona, where sufficient daytime excess PV energy exists, following the proposed cycling strategy can maximize monthly electricity bill savings by integrating PV, storage and grid power. Results of this experimentation on the prototype scale can be extended with suitable constraints and discounts to typical systems used on residential level.

Future scope for research in this regard will involve testing the proposed system with spring and fall loadshapes which would present a clear picture of yearly behavior of the battery assisted PV system. Critical battery performance issues such as ageing can be analyzed with this setup by cycling the battery for a year or two continuously thereby gathering a multiple year worth of data and assess the impact of ageing on cycle life and round-trip efficiency. Also a thorough cost benefit analysis could be carried out to account for capital, operational and replacement costs involved in the operational nexus of storage and PV.

VII. REFERENCES

[1] H. Beltran, M. Swierczynski et al. "Lithium ion batteries ageing analysis when used in a PV power plant," in 2012 IEEE International Symposium *on Industrial Electronics (ISIE),* pp. 1604-1609.

[2] R.L. Hammond, S. Everingham, Technical report on "Stationary batteries in cycling photovoltaic applications," [Online] Available at: http://www.battcon.com/PapersFinal2003/HammondPaperFINAL2003.pdf

[3] Li Yongdong, Rao Jianye, Sun Min, "Design and implementation of a solar array simulator," in *International conference on Electrical Machines and Systems 2008 (ICEMS),* pp. 2633-2636.

[4] C. Chang, E. Chang and H. Chang, "A high efficiency solar array simulator implemented by an LLC resonant DC-DC converter," *IEEE Transactions on Power Electronics*, Early Access Article

[5] E. Koutroulis, K. Kalaitzakis, V. Tzitzilonis, "Development of an FPGA-based system for real-time simulation of photovoltaic modules," in *17th IEEE International Workshop on Rapid System Prototyping 2006*, pp. 200-208.

[6] Agilent Technologies, datasheet on E4351B Solar Array Simulator Module [Online] Available: http://www.amdahl.com/doc/products /bsg/intra/ infra/html.

[7] Shen Weixiang, Bin, A.S.k, "Investigation of standalone photovoltaic systems," in *6th IEEE Conference on Industrial Electronics and Applications 2011 (ICIEA),* pp. 2651-2656.

[8] Shen Weixiang, A.S.kbin , O.K. Sen, "A study on standalone photovoltaic system with real meteorological data at Malaysia," in *8th IEEE Conference on Electrical Machines and Systems 2005 (ICEMS),* pp. 937-941, vol. 2.

[9] Mishra A., Irwin D, Shenoy P, Kurose J, Ting Zhu, " Smartcharge: Cutting the electricity bill in smart homes with energy storage," in *3rd International Conference on Future Energy Systems 2012,* pp.1-10.

[10] K. Alteneder (Salt River Project), notes on "Hourly seasonal demand data for SRP E-26 price plan," August 2011.

[11] Salt River Project (SRP),"Standard Electricity Price Plans," Corporate Pricing, [Online] Available at: http://www.srpnet.com/prices/pdfx/Standard_Electric_Price_Plans_May2012.pdf

[12] NREL, "National Solar Radiation Database (NSRDB)," [Online] Available at: http://rredc.nrel.gov/solar/old_data/nsrdb/

[13] Salt River Project (SRP),"Renewable Net Metering Rider," [Online] Available at: http://www.srpnet.com/environment/earthwise/pdfx/RenewNetMeterRider0510.pdf

VIII. BIOGRAPHIES

George G Karady (SM'70, F'78, LF 98) received his BSEE and Doctor of Engineering degree in electrical engineering from Technical University of Budapest. Dr. Karady is Power System Chair Professor at Arizona State University, where he teaches electrical power and performs research in Power Electronics, High Voltage Techniques and Electric Power Systems. Previously, he was with EBASCO Services where he served as Chief Consulting Electrical Engineer, Manager of Electrical Systems and Chief Engineer of Computer Technology. He also served as Electrical Task supervisor for the Tokomak Fusion Test reactor project at Princeton. Before that he worked for the Hydro Quebec Institute of Research as a Program Manager. Dr Karady started his career at Technology University of Budapest where he progressed from Post Doctoral Student to Deputy Department Head. Dr. Karady is a registered professional engineer in New York. He is the author of more than 200 technical papers. Dr. Karady is active in IEEE, he was chairman of Chapter/ Membership's Award Committee, Education committee's Award Subcommittee and WG on Non-ceramic insulators etc. Dr. Karady also served in the US National Committee of CIGRE as Vice President and Secretary Treasurer.

Aditya D. Nadkarni (S'12) received his B.Tech degree in Electrical Engineering from the University of Mumbai in 2010. He is currently working towards his M.S. degree at the Ira A. Fulton School of Electrical, Computer and Energy Engineering, Arizona State University in Tempe. Aditya's research interests include distributed generation, energy management systems and renewable grid integration.

Ken Alteneder works as Senior Principle Engineer at Salt River Project (SRP), Tempe in its distribution planning department.